Geologie en Mijnbouw **73:** 241–252, 1994.

What can we learn from aftershocks?

Frank Scherbaum
Institut für Allgemeine und Angewandte Geophysik, Ludwig Maximilians Universität, Theresienstr. 41, 80333 München, Germany

Received 23 April 1993; accepted in revised form 12 October 1993

Key words: stress changes, mainshock slip, waveform analysis, earthquake source

Abstract

From the spatial distribution of aftershocks with respect to the regions of fault slip during the mainshock, information can be gained about the heterogeneous structure within the source volume and about the frictional properties of surrounding faults. Focal mechanisms of aftershocks reveal how stress is redistributed by large earthquakes. While analog data have mainly been used for these studies in the past, a new degree of data quality is obtained with currently available digital recording systems. In addition to the increased accuracy for the determination of purely kinematic data, waveform information can be utilized with digital data. With state-of-the-art signal processing techniques, the contributions of source, path, and site effects on the observed seismic signals can be studied. Provided these effects can be separated, aftershock signals will potentially help us to learn about the properties of fault regions in unprecedented detail. The degree of resolution which can be achieved, however, will strongly depend on the number of stations and the geometry of the network employed. Depending on the special scientific problems to be addressed, optimum station geometries may vary. Modern methods in optimization theory, such as simulated annealing, have been successfully used to find optimum station distributions for aftershock monitoring. An additional aspect which has to be addressed is the problem of managing and processing aftershock data. Since high-quality digital data come at the price of huge data volumes, new strategies and concepts for data handling and signal processing have to be developed.

Introduction

In recent years, the seismological community has seen a growing number of initiatives for aftershock monitoring programs after large earthquakes. Aftershock studies in the past have contributed strongly to the understanding of the various factors contributing to the generation of earthquake damage and to the current concepts of earthquake faulting. In regions where faulting does not have any surface expression, the analysis of the spatial distribution of aftershocks may be the only way to obtain information on the location of the active faults. An example for the mapping of such 'blind' faults is the 1985 Kettleman Hills aftershock sequence in the eastern Californian Coast Range (Ekström et al. 1992).

Strong ground motion during large earthquakes is influenced by a variety of factors. Although initially controlled by complexities of the rupture process at the source, high-frequency seismic signals are distorted strongly by various effects during wave propagation. Due to the strong heterogeneities of the physical properties close to the earth's surface, site effects play a special role for the generation of damage. A complete understanding of all the contributing factors and their interaction is a truly interdisciplinary problem in which aftershock analysis can help to shed light on some of the seismological aspects.

One of the first properties of aftershock sequences that have been studied was the temporal behavior of their activity. Already around the turn of the century Omori recognized the fact that the activity rate $n(t)$ (numbers of events per time interval) could be described approximately by a power law ($n(t) = A\, t^{-p}$) (Omori 1894, 1900). This relationship was modified by Utsu (1961) to $n(t) = A\, (t + c)^{-p}$ and called mod-

ified Omori law, the name under which it is mainly known today. The scaling factor A will strongly depend on the magnitude of the mainshock. The larger the mainshock, the more aftershocks will occur. Finally, the factor c describes the rate at time $t = 0$. For Californian aftershock sequences, the exponent p seems to correlate with surface heatflow (Kisslinger & Jones 1991). An important consequence of the observation that aftershock decay rates seem to follow very well the modified Omori law could potentially concern the problem of predicting stronger aftershocks. One of the most promising precursory phenomena which have been proposed with some earthquakes in the past are changes in precursory seismic activity (e.g. Wyss 1991). A major problem in this context, however, is the determination of background seismicity rates against which potential anomalies have to be judged. Earthquake catalogues are known to be affected by numerous man-made factors which could easily cause spurious seismicity rate changes (e.g. Habermann 1987). This may be a severe problem for long-term observation during which network properties and procedures may change dramatically, but is less so for aftershock studies. In a study on precursory seismicity of strong aftershocks, Keilis-Borok et al. (1980) found that of 23 stronger aftershocks, 18 were preceded by anomalous seismicity rates. Other examples are given by Zhao et al. (1989), amongst them the aftershock sequences of the well known Haicheng (1975) and Tangshan (1976) earthquakes.

A study for the western U.S. showed that about 60% of all aftershocks occurred within 24 hours and about one third within a week of the mainshock, respectively (Doser 1989). For strong earthquakes, however, earthquakes may still have to be considered aftershocks one to two years after the mainshock (Gardner & Knopoff 1974). For the population in an earthquake disaster area, aftershocks are primarily a continuation of the threat. As a rule of thumb, it is often found that the magnitudes of the largest aftershocks reach up to about one magnitude unit below the mainshock.

The generation of aftershocks

The generation of aftershocks can be explained by a number of different mechanisms which in nature probably all act together. In Fig. 1, three different models are sketched schematically. In all conventional mainshock–aftershock interaction concepts, the mainshock rupture is thought to have caused local stress concentrations which are released by the aftershocks.

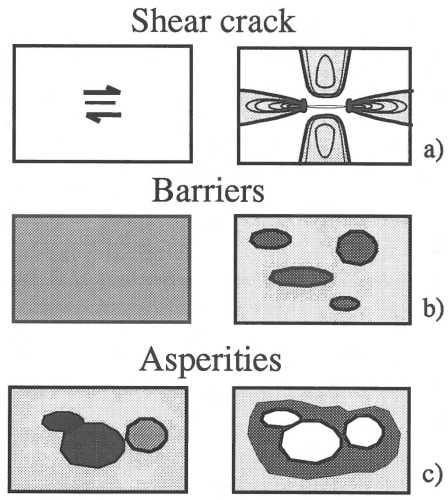

Fig. 1. Models for the generation of aftershocks. a) Shear crack (left-hand panel) with corresponding stress concentration (right-hand panel). b) Barrier model. Schematic stress distribution on the fault before (left-hand panel) and after (right-hand panel) the mainshock. The degree of shading indicates the level of stress. c) The same as in b) for the Asperity model.

Figure 1a shows a single shear crack which represents the main shock. This simple crack model predicts stress changes caused by the fault slip which yield a stress increase in the shaded areas. The stress increase is strongest at the crack tip, but it is also positive in the regions perpendicular to the crack. The unshaded region suffers a stress decrease. The models depicted in Figs 1b and 1c respectively, recognize the fact that fault zone heterogeneities in stress and/or strength play an important role in faulting. Shown is the stress distribution on the fault before and after the mainshock rupture, with darker shading indicating higher stresses. Most of the large earthquakes for which the slip distribution could have been determined, show a highly irregular slip pattern. Large earthquakes are often known to be so-called *complex events* in which the seismic energy is radiated from a number of different patches on the fault. These models are known as *barrier* and *asperity* models, respectively, depending on whether the complexity is mainly due to strength or to stress heterogeneities (e.g. Papageorgiou & Aki 1983a, b, Aki 1984, Papageorgiou 1985).

In the most simple form of the barrier model, the stress distribution before the mainshock is assumed to be uniform (Fig. 1b). During the mainshock, some patches on the fault zone (barriers) are left unbroken

while the rest of the fault slips and the stress is more or less released. With respect to the broken region of the fault, the unbroken patches are under higher stress which is released at a later time as aftershocks. In the asperity model, it is assumed that the stress distribution is heterogeneous before the mainshock, while the strength distribution is more or less uniform (Fig. 1c). During the mainshock, slip occurs on the patches of local stress concentrations (asperities). The area being under higher stress after the breakage of the asperities, will be the region surrounding the fracture surface. In Fig. 1c, this is indicated by three more or less connected asperities which are assumed to be under different stress before the mainshock. After the mainshock, the stress on the asperities is released and the surrounding area (shaded darker) is stressed and will become the region in which the aftershock activity will be concentrated. In one flavor of this model (Yamashita & Knopoff 1987), the main fracture surface is assumed to be surrounded by a large number of smaller cracks (satellite faults) slightly away from the fracture surface. Aftershock activity in this case would correspond to the breakage of the barriers between these satellite faults and the main rupture. The distinction between asperity and barrier model should be taken with a grain of salt. Barriers may become asperities at a later time in the faulting history and vice versa.

Independent of the way the aftershock generating stress concentrations are produced, all models in Fig. 1 have to employ a time-dependent strength mechanism in order to explain the temporal behavior of the activity. Again, there are a couple of ways how this can be achieved. From laboratory experiments it is well known that the rock strength can increase with strain rate. In the case of a mechanism called *dilatancy hardening*, for example, deformation causes an increase in pore space which will decrease the pore pressure. As long as the newly created void space is not filled by pore fluids, the rock will show a higher strength. In addition, it is known that rock and many other brittle materials will spontaneously fail after a characteristic time even if they are subject to stresses below their immediate breaking strength. This is called *static fatigue*. Both these mechanisms could explain the temporal behavior seen in Omori's law. A third mechanism which may contribute at least to some degree is the earthquake-induced fluid flow from regions of stress increase into regions of stress decrease. This will cause a time-dependent effective stress which under certain conditions can explain Omori's law. A review of these mechanisms can be found in the stimulating book 'The mechanics of earthquake faulting' by Scholz (1990).

While the importance of barriers and asperities for the faulting and especially for the generation of high frequency strong ground motion is well recognized, the physical properties of barriers and asperities are much less understood. Barriers for example could be regions of especially strong fault material and/or patches of small pore pressure. In addition they could simply correspond to geometric features such as fault bends or offsets (King 1986). Depending on which of the three mechanisms in Fig. 1 is controlling the mainshock rupture, the distribution of mainshock-induced stress should occur at different locations with respect to the rupture surface.

Aftershocks and mainshock slip spatial distribution

From the spatial distribution of various aftershock sequences for which the mainshock slip distribution could have been determined, a fairly consistent pattern in the spatial distribution of aftershocks is indicated. In many cases (Borah Peak 1983, North Palm Springs 1986, Imperial Valley 1979, Morgan Hill 1984, Loma Prieta 1989) the areas of low aftershock activity seem to correlate with the areas of high mainshock slip (Fig. 2, Mendoza & Hartzell 1988, Beroza 1990).

For the Borrego Mountain earthquake of 1968 and the Homestead earthquake of 1979 (Fig. 3), off-fault aftershock activity shows a pattern similar to what would be expected from the stress distribution after slip on a single large crack (Das & Scholz 1981, Stein & Lisowski 1983).

The story of the Homestead earthquake had a fascinating continuation in the form of the Landers earthquake of M_s = 7.4 of June 28, 1992, which was the largest earthquake to strike Southern California during the past four decades. Stein et al. (1992) calculated the changes in Coulomb failure stress caused by the four $M_L \geq 5.2$ earthquakes within 50 km of the Landers earthquake which occurred during the previous 17 years. The Homestead Valley earthquake of 1979 is one of them. They found that the Landers earthquake falls within a zone of elevated stress. Hence the stress changes caused by the Homestead event not only explain most of the spatial distribution of its aftershock activity, but together with other recent events in this area seem to have prepared for the Landers earthquake 13 years later. The same process of stress trans-

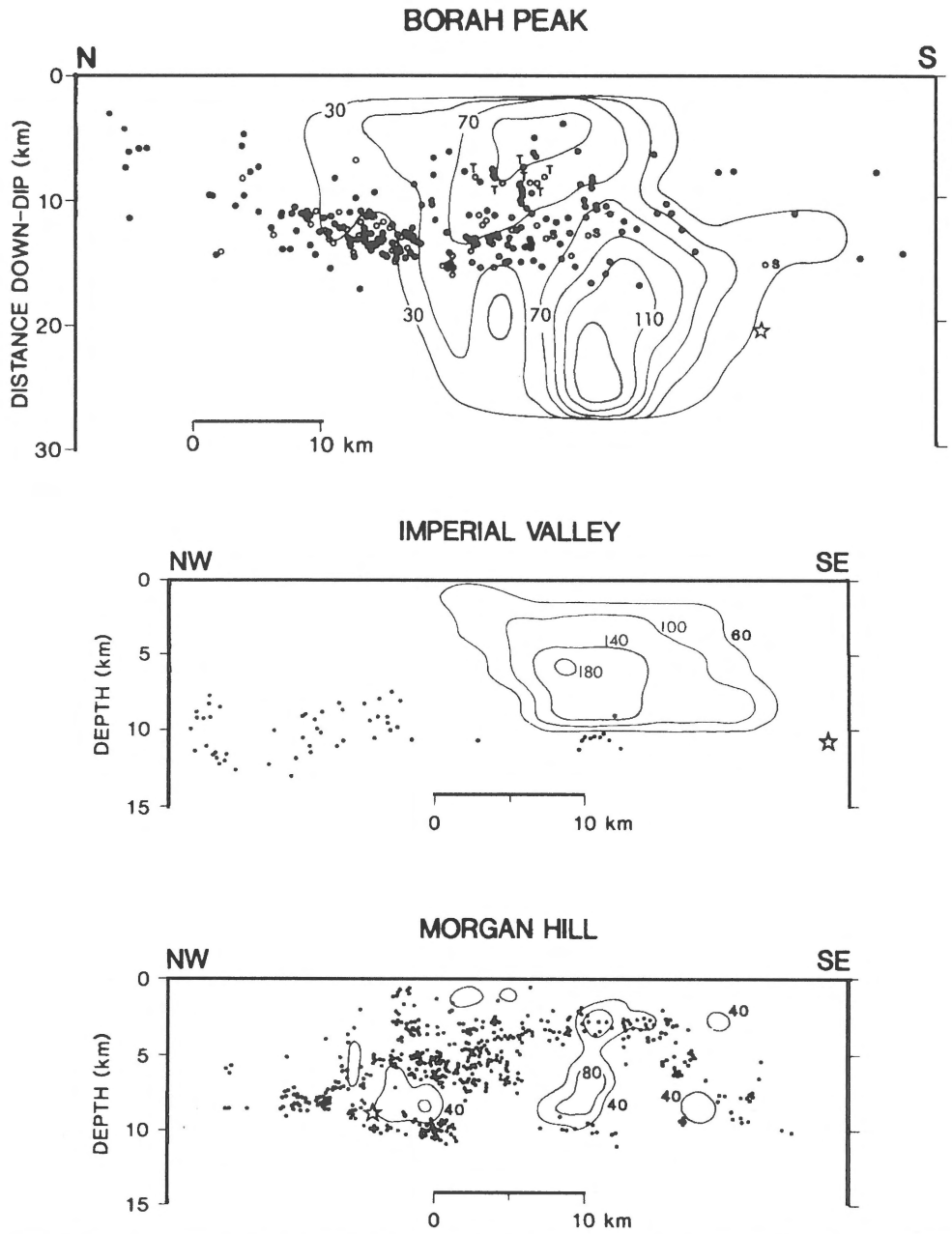

Fig. 2. Aftershock distribution (*open circles* and *black dots*) and contours of mainshock slip (in cm) for three large earthquakes in the US: the Boreah Peak, Idaho, normal dip-slip earthquake of October 28, 1983, the Imperial Valley, California, strike-slip earthquake of October 15, 1979, and the Morgan Hill, California, strike-slip earthquake of April 24, 1984. All hypocenters are projected on a vertical plane corresponding approximately to the mainshock rupture plane. Stars show mainshock hypocenter locations. Aftershock focal mechanisms are determined for the Boreah Peak earthquake (open circles: normal fault if not indicated, T – thrust, S – strike-slip). (From Mendoza & Hartzell 1988).

fer is seen with the apparent triggering of the Big Bear earthquake about $3^1/_2$ hours after the Landers event. The Landers event is predicted to have increased the proximity to failure at the Big Bear epicenter by about 3 bars (Stein et al. 1992).

A somewhat special case of mainshock–aftershock interaction seems to have happened in the case of the Loma Prieta earthquake of October 18, 1989 (M_s = 7.1). Judging from the spatial distribution of aftershocks with respect to the mainshock rupture, it looks

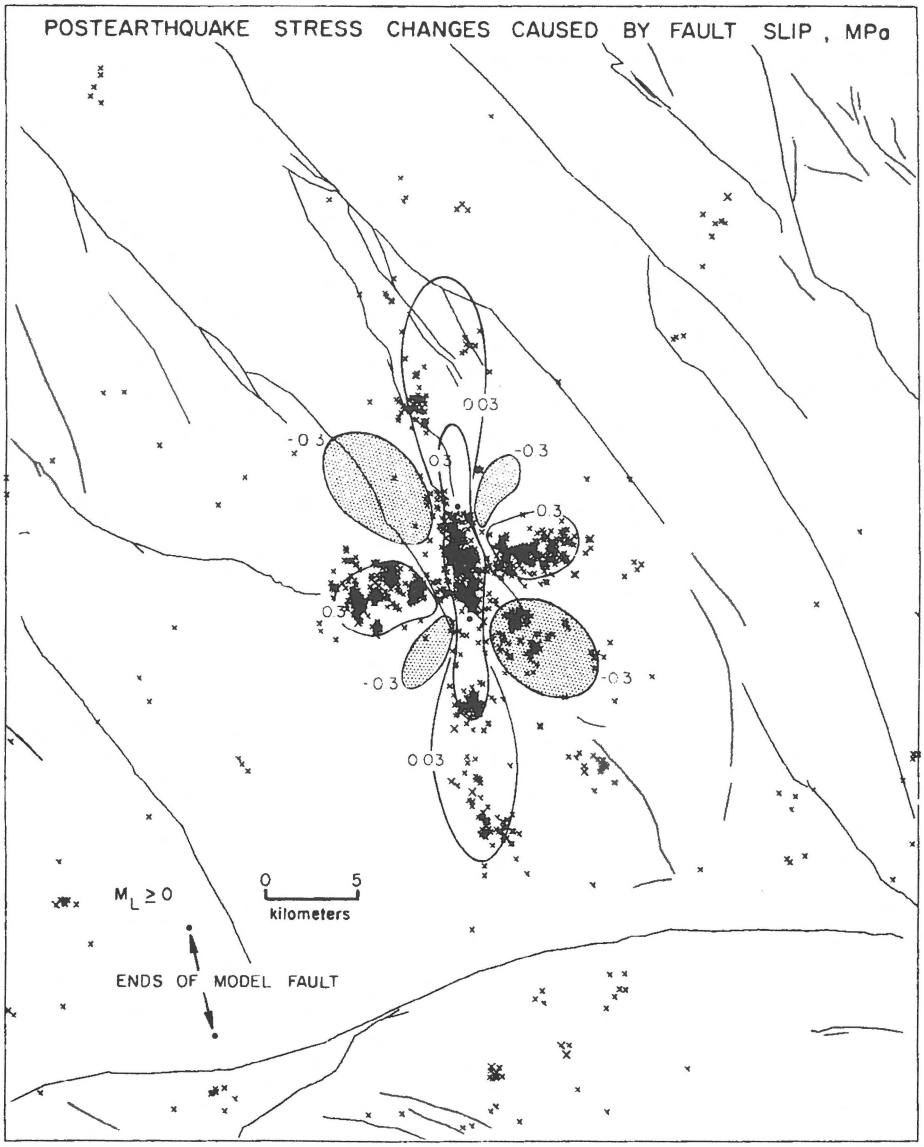

Fig. 3. Aftershock distribution for the 1979 Homestead Valley, California, aftershock sequence. The contours show the stress distribution from an essential N-S strike-slip fault. The shaded areas show regions of calculated stress decrease (from Stein & Lisowski 1983).

quite usual with the areas of high slip correlating well with the regions of low aftershock activity (Beroza 1990). However, as it was pointed out by Beroza & Zoback (1993), the focal mechanisms for these events are extremely diverse within very small volumes. This clearly is in conflict with the understanding that the aftershocks in general accommodate the mainshock-induced stress changes unless one would postulate an extremely heterogeneous stress distribution. However, looking at the different mechanisms as a function of strike for the strike-slip mechanisms and as a function of dip for the dip-slip mechanism, respectively, an interesting pattern emerges. Left-lateral events tend to strike more often at angles below 130°, while right-lateral events tend towards larger azimuths. For the dip-slip events, the normal faulting events more often have a dip above 70° while reverse faulting seems to happen preferably at lower dipping angles. If the aftershocks were to release mainshock-induced shear stress, the majority of the events should have a right-lateral focal mechanism. Instead, the aftershock mechanisms are consistent with a nearly uniaxial stress field in which

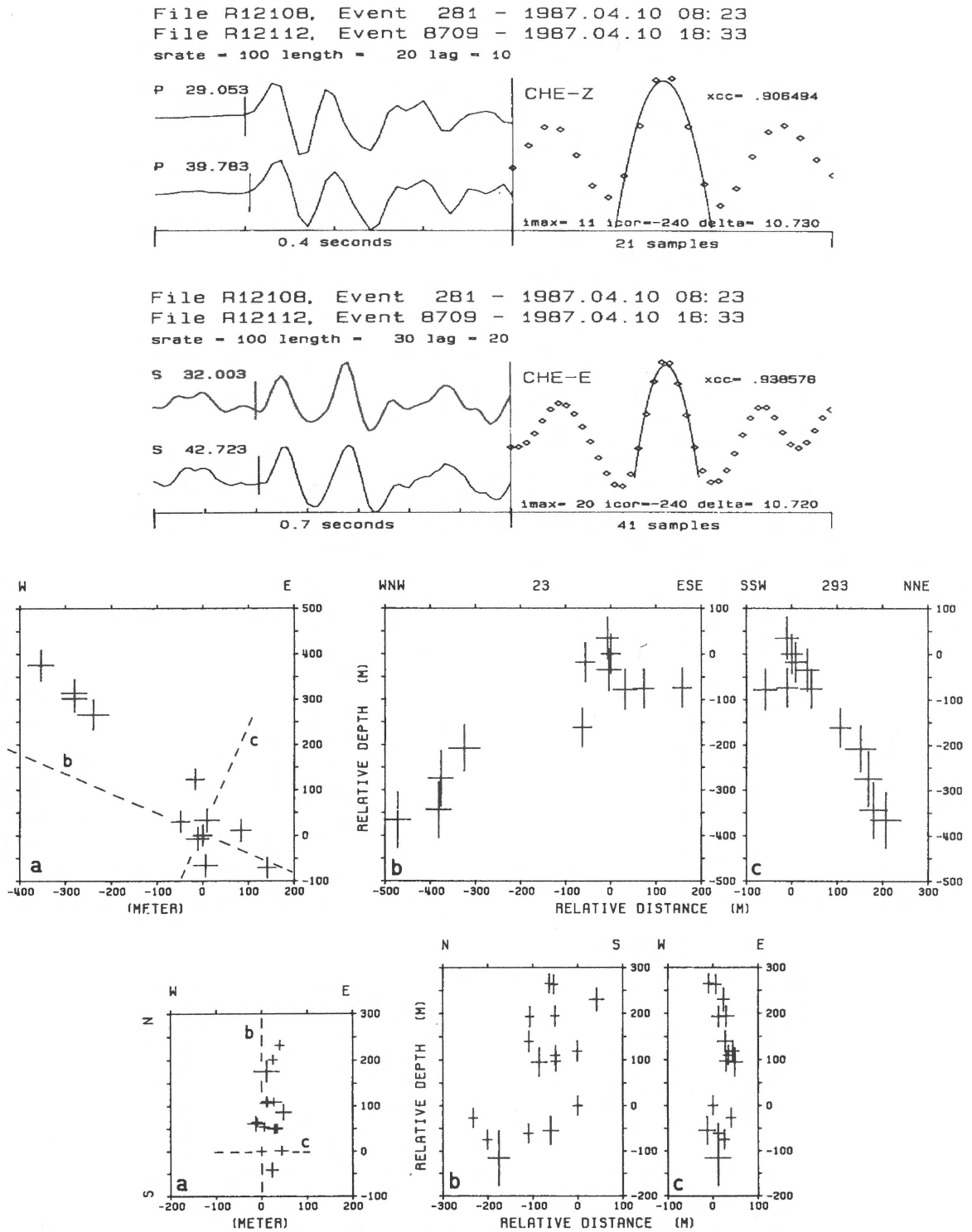

Fig. 4. Cluster analysis using cross-correlation for the determination of relative arrival times of coherent cluster signals is shown in the upper four panels. At the left the P-wave (P) and S-wave (S) traces are shown which are used in the cross-correlation, displayed at the right, for accurate relative arrival time determinations. Such an analysis is only possible for events with very similar waveforms, i.e. similar focal mechanisms and nearby locations. The relative locations obtained from the thus determined relative arrival times are shown in the bottom six panels for two clusters of small earthquakes in northern Switzerland. a) Maps showing relative locations of epicenters and lines of profiles in b) and c). b) and c) Relative locations of hypocenters in two perpendicular vertical planes. From Scherbaum et al. (1991).

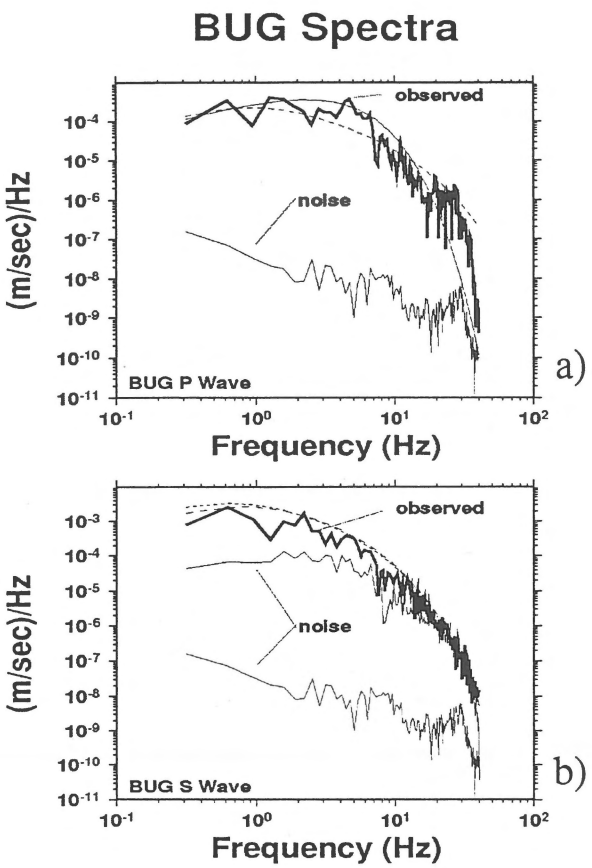

Fig. 5. P and S-wave spectra (of 3.2 sec ground velocity records) of the Roermond earthquake observed at station BUG of the German Regional Seismic Network. a) P-wave. The dashed line corresponds to $M_0 = 6.5\ 10^{10}$ Nm, $f_c = 1.0$ Hz, and a Q value of 500 (L. Ahorner, pers. comm.). The thin solid line shows the P-wave spectrum obtained from grid search using the noise level indicated (taken from before the P-wave onset). b) S-wave. The thin lines correspond to noise spectra taken from before the P-wave onset (lower noise level) and from the P-wave coda (higher noise level). The corresponding S-wave spectra found by grid search correspond to the long-dashed and short-dashed lines, respectively. The model parameters for the different spectral models vary between 0.5 and 10 Hz for the corner frequency and $5.4\ 10^{16} < M_0 < 15.9\ 10^{16}$ Nm, respectively.

the maximum principal stress acts perpendicular to the mainshock fault plane. This implies that the stress drop in the Loma Prieta mainshock was more or less complete. Additionally, the aftershock faults have to be extremely weak so that very little resolved shear stress on the fault planes results in rupture.

High-quality digital data analysis

All the aftershock parameters discussed so far, such as the hypocentral locations, the origin times and the focal mechanisms, can be obtained from purely kinematic data (onset times and polarities of certain phases). Adding amplitude data to an aftershock analysis, additional information of importance such as amplitude–distance relationships, which are, for example, required in the context of probabilistic seismic hazard analysis, can be obtained. Until recently, aftershock monitoring has been mainly done using analog recording systems. The availability of high-quality mobile digital recording systems has pushed the state of the art in aftershock studies to new limits. With high-quality digital data it is possible to address a completely new set of problems. In addition, the improved timing resolution of digital data provides the means to solve the basic problems such as earthquake location and the determination of focal mechanisms at much higher accuracies.

Knowing the spatial aftershock distribution is of great importance for the understanding of the stress changes caused by the mainshock. Fault zones, especially in interplate regions, show a high degree of heterogeneity. Applying a conventional location procedure with a one dimensional (1D) velocity structure may yield strongly biased hypocentral locations. Provided sufficient station coverage exists, tomographic imaging of the source region using aftershock signals can be used to obtain more accurate velocity structures for location (e.g. Thurber 1986, Kissling 1988, Eberhart-Phillips et al. 1990).

Even more details about the structure of a fault zone can be revealed from earthquakes which show some sort of clustering in space. In this case, the waveforms of the corresponding events often show a high degree of coherence. This similarity can be used to determine the relative arrival time differences of certain phases at very high accuracies (Ito 1985, Scherbaum & Wendler 1986, Scherbaum et al. 1991). The analysis of earthquake clusters using cross-correlation and/or cross-spectral techniques allows the determination of the structure of fault zones in unprecedented detail (Fig. 4).

Owing to the abundance of small events with high-frequency source signals, aftershock sequences provide a unique way of probing the source volume of a mainshock. Ultimately, the frequency contents of aftershock signals can tell a lot about the heterogeneous structure of the source region. However, from what is

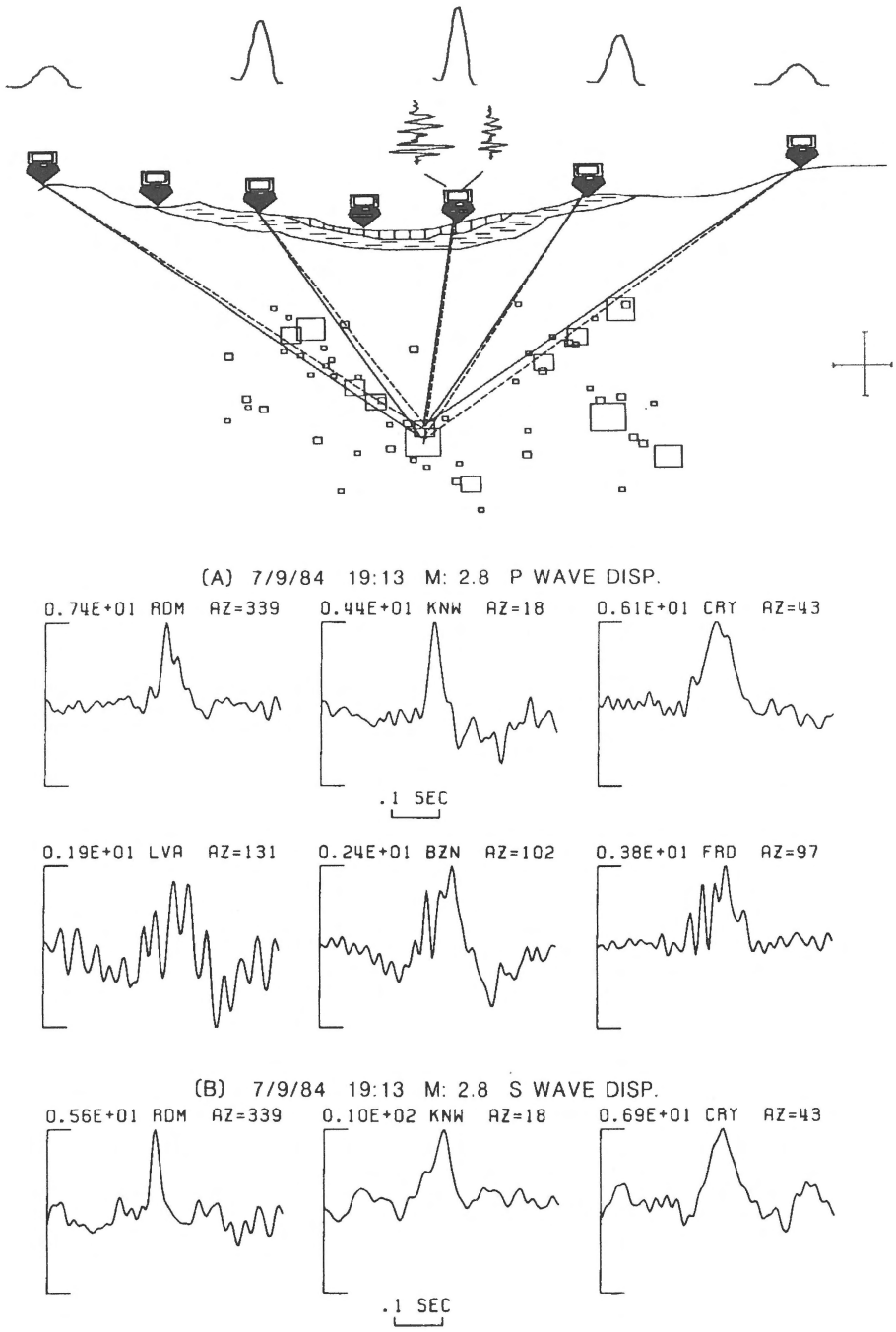

Fig. 6. The principle of source imaging using doublet earthquakes. The top panel illustrates the recording geometry (from Steinwachs & Scherbaum 1991), while the bottom panel shows the resulting source time function for a southern California doublet event derived for P-wave and S-wave signals recorded at different stations and epicentral azimuths (AZ) (from Frankel et al. 1986).

known about the interaction between the source signals and the propagation medium, it has to be kept in mind that the seismic signals recorded at the earth's surface have been distorted by many different filtering effects. Due to the various effects of attenuation, modelling earthquake spectra with single station records is a strongly non-unique problem (Scherbaum 1990). As an example for this ambiguity, Fig. 5 shows different

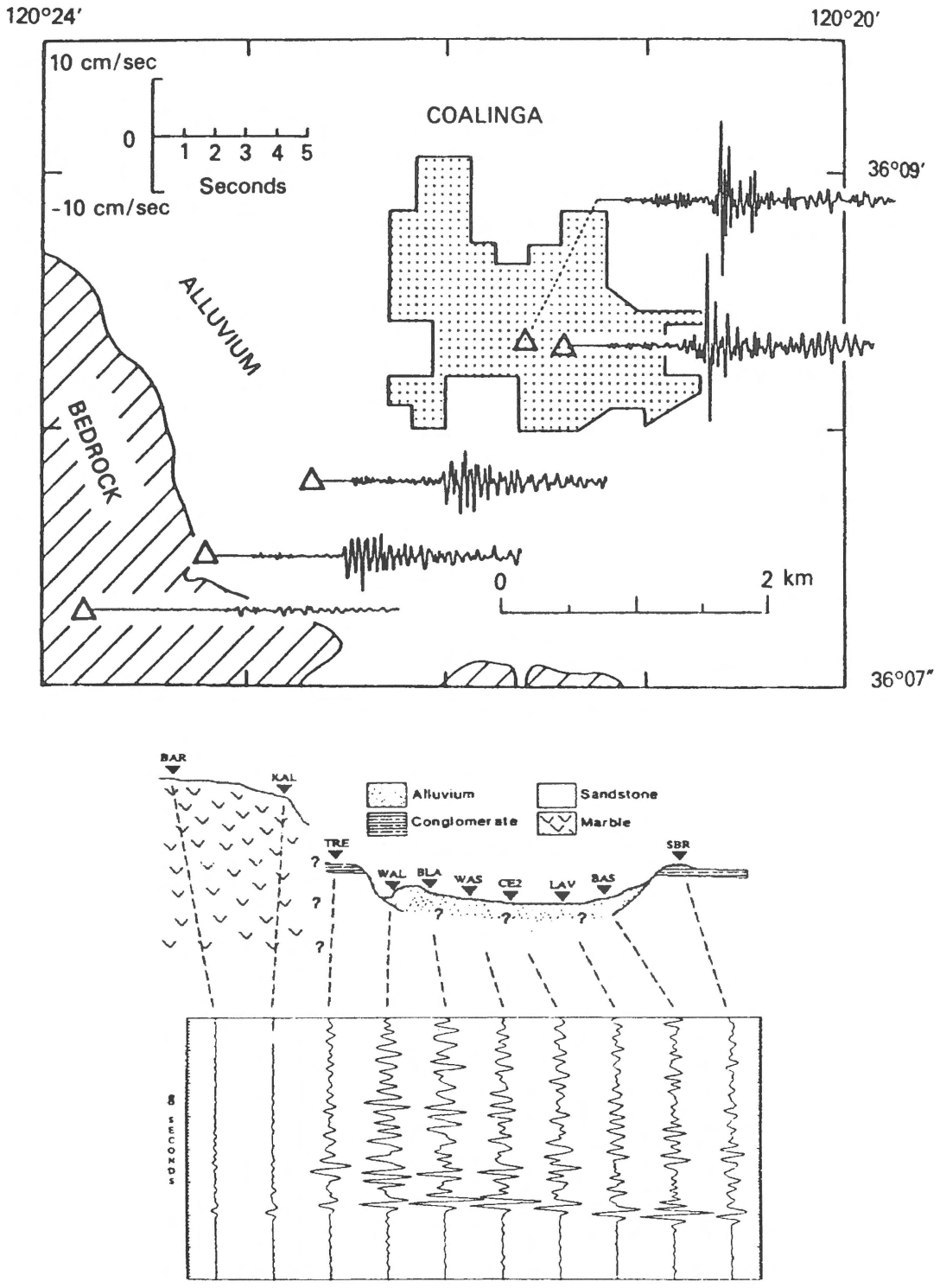

Fig. 7. Mapping out site amplifications using aftershock recordings. The top panel (from Reiter 1990) shows the site-specific records for a magnitude 4.3 aftershock of the 1983 Coalinga, California, earthquake. The bottom panel shows an aftershock of the 1989 Loma Prieta, California, earthquake recorded in down-town Santa Cruz. Note the differences in amplitudes as well as in strong motion durations.

spectral models to fit the observed S-wave spectrum of the Roermond mainshock at the German Regional Station Network (GRSN) station Bochum (BUG), approximately 100 km away.

While this problem cannot be overcome with single station analysis, some of the ambiguities can be constrained with well-distributed networks and well-distributed events by simultaneously determining the attenuation structure and the spectral parameters (Scherbaum 1990). As a result, 3D images of the attenuation structure as well as the spatial distribution of high-frequency radiation from the source volume can be obtained (Scherbaum & Wyss 1990).

A different way to work around the problem of signal distortion due to propagation effects is by using events which have occurred essentially at the same location at different times. The signal differences at a given station for these *doublets* are purely due to source effects. Hence, the signal of the smaller event of a doublet can be used as a Green's function and can be deconvolved from the signal of the larger event. The resulting signal will be an approximation to the source signal of the larger event (Fig. 6, Frankel et al. 1986).

A very special role in the context of the generation of damage during large earthquakes is known to be played by the effects of the local site (e.g. Plafker & Galloway 1989, Beck & Hall 1986). Mexico City is one of the best known examples for this kind of interactions. Although the effects have been known for a long time, not all of the contributing factors are fully understood. Aftershock sequences can be used to map out areas of potential site amplification, which is extremely important for the future hazard evaluation (Fig. 7).

With the advent of new discrete optimization techniques such as simulated annealing and genetic algorithms, we may even be able in the future to obtain automatically site-specific layer models from aftershock recordings. As an example for this type of approach, Fig. 8 shows a preliminary six-layer S-wave site model for the University of Cologne station SBR (Schalbruch) which was obtained automatically using a genetic algorithm modelling approach. In the top panel you see the observed seismogram superimposed by the synthetic one corresponding to the site model in the lower panel.

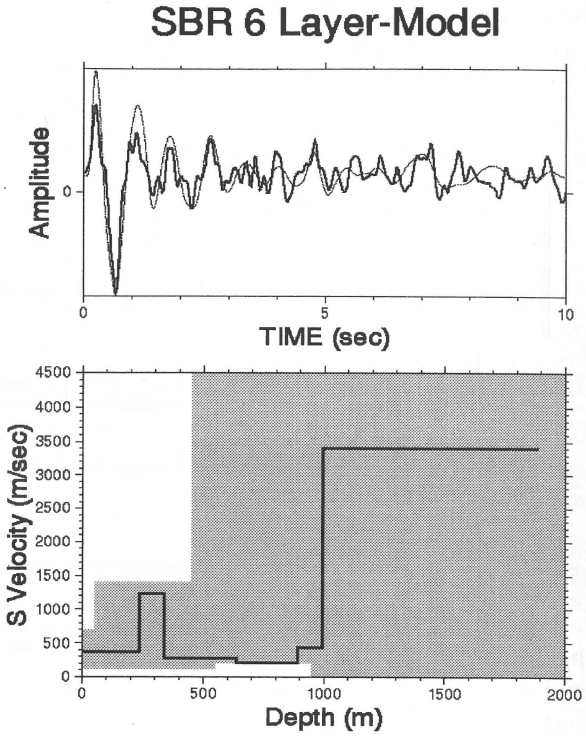

Fig. 8. Automatic site modelling using genetic algorithm search. This example shows a preliminary S-wave six-layer velocity model for station SBR (Schalbruch, University of Cologne). In the upper panel the seismogram (solid curve) of a Roermond aftershock has been provided by L. Ahorner. The modelled seismogram (thin line) has been obtained using the velocity model (solid line) shown in the lower panel. The shaded area in the lower panel indicates the region in which the velocity – depth model was allowed to vary.

Conclusions

Aftershocks are clearly an extremely important source of information, which can be utilized for the reduction of the vulnerability to future earthquakes. Recording aftershocks can help to understand the generation of damage and the interaction of the various contributing factors such as the effects of the source, propagation medium and the local site conditions. While numerous important contributions along these lines have already been made using existing methods and know-how, certain issues will need increased attention in the future in order to make full use of the potential contained in aftershocks.

Systematic state-of-the-art waveform analysis on aftershock data consists of many interrelated steps and requires huge amounts of data to be 'touched' many times. Hence, we will have to learn how to deal with huge waveform volumes in a clever way. Whether we

like it or not, we will have to make use of automated or semi-automated methods at least for a quick analysis. To make this really work it will also require some re-thinking of the ways we look at seismic signals in terms of parametrization of signal parameters (e.g. wavelet transforms, etc.).

One question that requires considerable attention is the design of the mobile seismic networks used for aftershock monitoring. One obvious problem is the design of the hardware–software interface. With the huge amount of data which has to be collected for aftershock waveform studies, the way data are produced cannot be decoupled conceptually any longer from the way the data are processed. This is a point I believe where hardware manufacturers are challenged. On the other hand there is also the problem of network geometry. It is well known that the quality of a network for whatever task considered strongly depends on its geometry. This becomes especially complicated when keeping in mind that off-fault events may be the most interesting events in terms of constraining the stress transfer during the mainshock. Simulated annealing has been found to perform very well for the problem of finding optimum station distributions for aftershock recordings under a variety of constraints (Scherbaum & Hardt 1992, Hardt & Scherbaum 1994).

Finally, I want to stress the point that for the generation of earthquake disasters, the seismological aspect is just one amongst many other factors that have to be understood better. Understanding the generation of earthquake disasters in total requires interaction between many different fields, ranging from geosciences, soil dynamics, structural engineering to even social sciences. And since earthquakes don't care about political boundaries, we also need to strengthen international cooperation in this field.

References

Aki, K. 1984 Asperities, barriers, characteristic earthquakes and strong ground motion prediction – J. Geophys. Res. 89: 5867–5872

Beck, J.L. & J.F. Hall 1986 Factors contributing to the catastrophe in Mexico City during the earthquake of September 19, 1985 – Geophys. Res. Lett. 13: 593–596

Beroza, G.C. 1990 Near-source modeling of the Loma Prieta earthquake: evidence for heterogeneous slip and implications for earthquake hazard – Bull. Seismol. Soc. Am. 81: 1603–1621

Beroza, G.C. & M.D. Zoback 1993 Mechanism diversity of the Loma Prieta aftershocks and the mechanics of mainshock-aftershock interaction – Science: 259: 210–213

Cranswick, E., K.W. King, P. Spudich, D.L. Carver, D.M. Worley & R. Banfill 1990 Site response across the downtown Santa Cruz alluvial basin – EOS 71: 287

Das, S. & C. Scholz 1981 Off-fault aftershock clusters caused by shear stress increase – Bull. Seismol. Soc. Am. 71: 1669–1675

Doser, D.I. 1989 Foreshocks and aftershocks of large (M = 5.5) earthquakes within the Western Cordillera of the United States – Bull. Seismol. Soc. Am. 80: 110–128

Eberhart-Phillips, D., V.F. Labson, W.D. Stanley, A.J. Michael & B.D. Rodriguez 1990 Preliminary velocity and resistivity models of the Loma Prieta earthquake region – Geophys. Res. Lett. 17: 1235–1238

Ekström, G., R.S. Stein, J.P. Eaton & D. Eberhart-Phillips 1992 Seismicity and geometry of a 110-km long blind thrust fault 1. The Kettleman Hills, California, Earthquake – J. Geophys. Res. 97: 4843–4864

Frankel, A., J. Fletcher, F. Vernon, L. Haar, J. Berger, T. Hanks & J. Brune 1986 Rupture Characteristics and Tomographic Source Imaging of ML~3 Earthquakes Near Anza, Southern California – J. Geophys. Res. 91: 12633–12650

Gardner, J.K. & L. Knopoff 1974 Is the sequence of earthquakes in southern California with aftershocks removed Poissonian? – Bull. Seismol. Soc. Am. 64: 1363–1367

Habermann, R.E. 1987 Man-made changes of seismicity rates – Bull. Seismol. Soc. Am. 77: 141–159

Hardt, M. & F. Scherbaum 1994 The design of optimum networks for aftershock recordings – Geophys. J. Intern. 117: 716–726

Ito, A. 1985 High Resolution relative hypocenters of similar earthquakes by the cross-spectral analysis method – J. Phys. Earth 33: 279–294

Keilis-Borok, V.I., L. Knopoff & I.M. Rotvain, 1980 Bursts of aftershocks, long-term precursors of strong earthquakes – Nature 283: 259–263

King, G.C.P. 1986 Speculations on the geometry of the initiation and termination processes of earthquake rupture and its relation to morphology and geological structure – Pageoph. 124: 567–585

Kissling, E. 1988 Geotomography with local earthquake data – Rev. Geophys. 26: 659–698

Kisslinger, C. & L.M. Jones 1991 Properties of aftershock sequences in Southern California – J. Geophys. Res. 96: 11947–11958

Mendoza, C. & S.H. Hartzell 1988 Aftershock patterns and main shock faulting – Bull. Seismol. Soc. Am. 78: 1438–1449

Omori, F. 1894 On aftershocks (in Japanese) – Rep. Imp. Earthq. investig. Comm. 2: 103–109

Omori, F. 1990 Investigation of aftershocks (in Japanese) – Rep. Imp. Earthq. investig. Comm. 30: 4–29

Papageorgiou, A.S. & K. Aki 1983a A specific barrier model for the quantitative description of inhomogeneous faulting and the prediction of strong ground motion, I. Description of the model – Bull. Seismol. Soc. Am. 73: 693–722

Papageorgiou, A.S. & K. Aki 1983b A specific barrier model for the quantitative description of inhomogeneous faulting and the prediction of strong ground motion, Part II. Applications of the model – Bull. Seismol. Soc. Am. 73: 953–978

Papageorgiou, A.S. 1985 Barrier and Asperity models of strong ground motion. In: R.E. Scholl & J.L. King (eds), Strong Ground Motion Simulation and Earthquake Engineering Applications. Earthq. Eng. Res. Inst., El Cerrito, CA, Publ. 85-02: 15-1–15-9

Plafker, G. & J.P. Galloway (eds) 1989 Lessons learned from the Loma Prieta, California, Earthquake of October 17, 1989, U.S. Geol. Survey Circ 1045

Reiter, L. 1990 Earthquake Hazard Analysis – Colombia University Press, New York, 254 pp

Scherbaum, F. & J. Wendler 1986 Cross spectral analysis of Swabian Jura, SW Germany, Three component microearthquake records – J. Geophys. 60: 157–166

Scherbaum, F. 1990 Combined Inversion for the Three-dimensional Q structure and source parameters using microearthquake spectra – J. Geophys. Res. 95: 12423–12438

Scherbaum, F. & M. Wyss 1990 Distribution of Attenuation in the Kaoiki, Hawaii, Source Volume estimated by inversion of P-Wave Spectra – J. Geophys. Res. 95: 12439–12448

Scherbaum, F., D. Gillard & N. Deichmann 1991 Slowness Power Spectrum Analysis of the Coda Composition of two Microearthquake Clusters in Northern Switzerland – Phys. Earth Planet. Inter. 67: 137–161

Scherbaum, F. & M. Hardt 1992 Optimizing the station distribution of seismic networks for aftershock recordings by simulated annealing – Cah. Centre Eur. Géodyn. Séismol. 6: 237–251

Scholz, C.H. 1990 The mechanics of earthquake faulting – Cambridge University Press, 439 pp

Stein, R.S. & M. Lisowski 1983 The 1979 Homestead Valley earthquake sequence, California: control of aftershocks and postseismic deformation – J. Geophys. Res. 88: 6477–6490

Stein, R.S., G.C.P. King & J. Lin 1992 Change in failure stress on the Southern San Andreas Fault System caused by the 1992 Magnitude = 7.4 Landers Earthquake – Science, 258: 1328–1332

Steinwachs, M. & F. Scherbaum 1991 Ursachenforschung bei Erdbebenkatastrophen. In: P. Knoll & D. Werner (eds), Proc. Koll. Erdbebeningenieurwesen, Potsdam 1991, DGEB – Publ. 5: 93–119

Thurber, C.H. 1986 Analysis methods for kinematic data from local earthquakes – Rev. Geophys. 24: 793–805

Utsu, T. 1961 A statistical study on the occurrence of aftershocks – Geophys. Mag. 30: 521–605

Wyss, M. (ed.) 1991 Evaluation of proposed earthquake precursors – American Geophysical Union, Washington, D.C., 94 pp

Yamashita, T. & L. Knopoff 1987 Models of aftershock occurrence – Geophys. J.R. Astr. Soc. 91: 13–26

Zhao, Z., K. Matsumura & K. Oike 1989 Precursory change of aftershock activity before large aftershocks: A case study for recent earthquakes in China – J. Phys. Earth 37: 155–177